(1970).
[19]J. Tauc, A. Menth, and D. L. Wood, Phys. Rev. Letters 25, 749 (1970).
[20]S. C. Moss and J. F. Graczyk, Phys. Rev. Letters 23, 1167 (1969).
[21]J. W. Osmun and H. Fritzsche, Appl. Phys. Letters 16, 87 (1970).
[23]T. Donovan (private communication).
[22]T. M. Donovan, E. J. Ashley, and W. Spicer, Phys. Letters 32A, 85 (1970).
[24]R. Y. Koyama, thesis, Technical Report No. 5223-1, Appendix 1 (Stanford University, (1969) (unpublished).
[25]D. E. Polk, J. Non-Cryst. Solids 5, 365 (1971).
[26]R. N. Stuart and F. Wooten, Phys. Rev. 156, 364 (1967).
[27]H. R. Philipp and H. Ehrenreich, Phys. Rev. 129, 1550 (1963).
[28]E. O. Kane, Phys. Rev. 127, 131 (1962).
[29]J. Ballantyne, Phys. Rev. (to be published).

PHYSICAL REVIEW B VOLUME 4, NUMBER 12 15 DECEMBER 1971

# Excitonic Theory of Electroabsorption: Phonon-Assisted Indirect Transitions in Si and Ge†

Binneg Y. Lao,* John D. Dow, and Frank C. Weinstein‡
*Joseph Henry Laboratories of Physics, Princeton University, Princeton, New Jersey* 08540
(Received 9 July 1971)

The theory of indirect phonon-assisted optical absorption by semiconductors in a uniform electric field is developed with particular attention being paid to the effects of electron-hole correlations (excitons). The Coulombic electron-hole interaction is treated within the Wannier-exciton effective-mass approximation. The physics of indirect electroabsorption is discussed, and it is found that exciton theory predicts an indirect absorption spectrum which is dramatically different, both qualitatively and quantitatively, from the spectrum predicted by one-electron theory (neglecting electron-hole correlations). The excitonic correlations are responsible for four qualitative features found in measured differential electroabsorption spectra but omitted by the one-electron theory: (i) The threshold for optical absorption by excitons lies at a lower energy; (ii) excitons cause a sharp drop on the high-energy side of the first differential electroabsorption peak; (iii) the amplitude of the differential absorption is enhanced by excitons; and (iv) excitonic spectra exhibit longer periods of spectral oscillations. These excitonic effects are analogous to effects previously predicted for direct transitions. Numerical calculations of the differential electroabsorption at the indirect edges of Ge and Si are compared with the data of Frova *et al.* and are found to be in excellent agreement with experiment.

## I. INTRODUCTION

In recent years, modulation spectroscopy[1] has become one of the most powerful tools for probing the electronic states of solids. In the area of electric field modulation experiments, in which the spectra are obtained by measuring the response of a semiconducting solid to an external square-wave-modulated electric field, differential absorption measurements have been reported for both direct- and indirect-band-gap semiconductors.[2] Until recently, the theoretical treatments of electroabsorption data have been limited to the one-electron approximation,[3] which neglects the excitonic correlations between the positions of the optical electron and hole. These correlations, caused by the final-state Coulomb interaction between the electron and the hole, lead to the formation of bound and continuum states of the exciton, and significantly change the shape of absorption spectra from that predicted by one-electron theory.

The importance of the final-state interactions on measured spectra was recognized several years ago,[2] but the theory of electroabsorption has only recently become sufficiently sophisticated[4-6] to evaluate these correlation effects. In this paper we report the first calculations[7] to go beyond the one-electron approximation and to include electron-hole correlations in the evaluation of the differential electroabsorption coefficient at an indirect edge. We use these results to analyze the indirect electroabsorption data for Ge and Si measured by Frova, Handler, Germano, and Aspnes.[2]

One purpose of these calculations is to test the validity of the Elliott theory[8] of absorption by excitons in indirect phonon-assisted optical transitions. Such transitions in Ge and Si represent an ideal test of the theory because (i) energy conservation forbids many of the broadening processes that tend to complicate the spectra at higher optical thresholds, (ii) the energy-band structures are well known for these materials,[9] and (iii) the absorption coefficient is sufficiently small to guarantee that most of the absorption occurs in the

bulk of the solid, free of the inhomogeneities associated with the surface. Our calculations are compared with the experimental data of Frova *et al.*[2] On the basis of these comparisons we are able to conclude that the Elliott theory of absorption by excitons plus a phenomenological broadening of the theoretical differential absorption curve $\Delta\alpha(\omega)$ are all that are needed to describe the indirect electroabsorption spectra in these materials. Higher-order many-body or local-field correlations are unnecessary to fit the data and, therefore, are uncalled for at the present.

The importance of exciton effects on a differential spectrum is highlighted by the fact that the measured differential absorption coefficient $\Delta\alpha(\omega, F)$ is a small difference between the finite-field $[\alpha(\omega, F)]$ and zero-field absorption coefficients $[\alpha(\omega, 0)]$. Therefore, exciton effects in the zero-field absorption spectrum alone manifest themselves as significant deviations of the measured spectrum from the predictions of one-electron theory. As an example, we note that the zero-field absorption threshold has a $\delta$-function (square-root) dependence on energy for direct (indirect) exciton transitions at an $M_0$ critical point as shown by Elliott theory,[8] in contrast to the square-root (square) dependence of one-electron theory. These more abrupt thresholds have both been observed experimentally.[10,11] In addition, we shall see that the electron-hole interaction significantly alters the free-electron prediction for finite-field absorption as well, leading to a theoretical differential spectrum $\Delta\alpha(\omega)$ which is both qualitatively and quantitatively different from the uncorrelated one-electron spectrum.

The calculations of excitonic indirect electroabsorption presented here extend the one-electron theories[3] of Penchina, Chester and Fritsche, and Aspnes to include electron-hole correlation; the computations are complementary to our previous work[12] on the effects of excitons on direct optical transitions in a uniform electric field. There we showed that the final-state Coulomb interaction produced four noticeable differences from the predictions of the one-electron Franz-Keldysh theory of differential electroabsorption: (i) The band-gap energy is noticeably higher; (ii) the zero-field exitons contribute a dominant negative peak; (iii) the amplitude of the different signal is greatly enhanced; and (iv) the periods of spectral oscillation are longer. Analogs of these four exciton effects at the direct edge appear in the indirect spectra. In the related area of differential electroreflectance, Weinstein, Dow, and Lao[13] showed recently that a comparison of exciton theory with experimental data gives an accurate value of the direct optical transition matrix element in Ge and leads to a fit which is better than that provided by one-electron theory, especially near the band edge where the differential absorption is strongest and the parabolic-band effective-mass approximation is expected to be valid. The present work also produces excellent agreement between theory and experiment.

Section II of this paper is devoted to a discussion of qualitative features that tend to show up in indirect electroabsorption spectra as a result of the Coulomb interaction between the electron and the hole. Section III contains an outline of the exciton theory of indirect optical transitions using a second-quantized formalism. Numerical techniques necessary to obtain the calculated spectra are discussed in Sec. IV. In Sec. V we present the results and a comparison with experiment; the discussion of these results is given in terms of the qualitative features presented in Sec. II. Our conclusions are presented in Sec. VI.

## II. QUALITATIVE CONSIDERATIONS

Before we deal with the formal theory of differential electroabsorption by indirect transitions, we first point out those qualitative features of theoretical indirect electroabsorption spectra which distinguish exciton theory from one-electron theory. Once the qualitative features associated with excitons are understood, it is relatively easy to identify exciton-related structures in measured spectra; thus the process of fitting theory to experiment is greatly simplified.

The physics of indirect differential electroabsorption is contained in Eqs. (3.35), relating the differential absorption coefficient to the exciton envelope wave function[14]:

$$\Delta\alpha(\omega) \equiv \alpha(\omega, F) - \alpha(\omega, 0)$$
$$= \sum_v \tilde{D}_v (2M_v/\hbar^2)^{3/2} \int_{-\infty}^{E_0} dE\, \Delta[|U_E(0)|^2 S(E)] \times (\hbar\omega \mp \hbar\Omega_{\vec{K}_m} - E_{gap} - E)^{1/2}, \quad (2.1)$$

where

$$\Delta[|U_E(0)|^2 S(E)] = |U_{E,F}(0)|^2 S(E) - |U_{E,0}(0)|^2 S(E) \quad (2.2a)$$

and

$$E_0 = \hbar\omega \mp \hbar\Omega_{\vec{K}_m} - E_{gap}\,. \quad (2.2b)$$

Here $\tilde{D}_v$ is the constant defined in Eq. (3.35b) and involves the transition matrix element and the electron-phonon coupling strength. $M_v$ is the effective mass of the electron plus that of the hole in valence band $v$; $v$ takes on the values 1 or 2 referring to light- and heavy-mass valence bands, respectively; $\hbar\Omega_{\vec{K}_m}$ is the energy of the phonon responsible for the indirect transition; the upper and lower signs refer, respectively, to one such

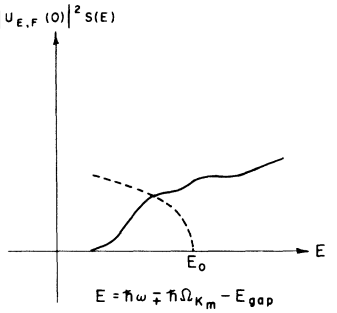


FIG. 1. Illustrating the convolution procedure. An arbitrary absorption strength $|U_E(0)|^2 S(E)$ as a function of $E$ is plotted (solid line). The corresponding indirect absorption coefficient $\alpha(\omega)$ at frequency $\omega$, where $E_0 = \hbar\omega \mp \hbar\Omega_{\vec{K}_m} - E_{gap}$, can be obtained by convoluting $|U_E(0)|^2 S(E)$ with the square-root function $(E_0 - E)^{1/2}$ (shown as the dashed line on the figure).

phonon created or absorbed in the optical absorption process. $E_{gap}$ is the energy gap between the top of the valence band and the minimum of the indirect conduction band; $S(E)$ is the density of internal-motion states of the exciton; and $U_{E,F}(0)$ is the wave amplitude at the origin of the electron-hole envelope function, thus $U_{E,F}(\vec{r})$ solves the hydrogenic relative-motion Schrödinger equation of the exciton

$$\left(-\frac{\hbar^2}{2\mu}\nabla^2 - \frac{e^2}{\epsilon_0 r} - eFz\right) U_{E,F}(\vec{r}) = E U_{E,F}(\vec{r}) \ . \tag{2.3}$$

Here $\mu$ is the reduced mass of the electron and hole, $\epsilon_0$ is the static dielectric constant, $F$ is the applied electric field (assumed uniform and directed along the $z$ axis), $e$ is the electron's charge, $\hbar$ is Planck's constant divided by $2\pi$, and $E$ is the internal energy of the exciton. The symbol $\Delta$ indicates the change induced by application of an external electric field $F$ as shown in Eq. (2.2a). Equation (2.1) also holds without the $\Delta$ symbol, thus we have

$$\alpha(\omega, F) = \sum_v \tilde{D}_v \left(\frac{2M_v}{\hbar^2}\right)^{3/2} \int_{-\infty}^{E_0} dE \, |U_{E,F}(0)|^2 S(E) \times (\hbar\omega \mp \hbar\Omega_{\vec{K}_m} - E_{gap} - E)^{1/2} \ . \tag{2.4}$$

It is very easy to understand the basic physics of this equation. $|U_{E,F}(0)|^2 S(E)$, henceforth referred to as the *absorption strength*, is the probability of finding the electron and the hole in the same unit cell multiplied by the density of states. When the exciton has energy $E$ in its relative (internal) motion, the rest of the energy of the absorbed photon $\hbar\omega \mp \hbar\Omega_{\vec{K}_m} - E_{gap} - E$ is available for center-of-mass motion of the exciton. From phase-space considerations, the density of states provided by the center-of-mass motion is just $(2M_v/\hbar^2)^{3/2}(\hbar\omega \mp \hbar\Omega_{\vec{K}_m} - E_{gap} - E)^{1/2}$. Equation (2.4) immediately follows. The convolution procedure by a square root is illustrated in Fig. 1.

Before we discuss the difference in $\alpha(\omega)$ induced by a finite field $F$, it is instructive to investigate the behavior of the derivatives of $\alpha(\omega, F)$ with respect to photon energy and field, evaluated at zero applied field. This is done in the Appendix. In contrast with one-electron theory (which predicts a square-root absorption strength, a quadratic indirect absorption, a linear energy derivative $\delta\alpha/\delta\hbar\omega$, and an exponential small-field derivative $\delta\alpha/\delta F$), exciton theory predicts an absorption threshold behavior dominated by the 1$s$ exciton $\delta$-function absorption strength, square-root indirect absorption, singular inverse square root $\delta\alpha/\delta\hbar\omega$, and singular first derivative $\delta\alpha/\delta F$—all a result of the quadratic Stark shift of the 1$s$ exciton. Some of these results are plotted in Ref. 15. Thus the excitons dramatically alter the nature of the small-field indirect electroabsorption spectrum near threshold.

For larger fields,[16] $\Delta\alpha(\omega)$ can no longer be easily evaluated in terms of its derivatives, and furthermore the Stark broadening of the exciton lines becomes more important than the Stark shift. Thus it is necessary to evaluate $\Delta\alpha(\omega)$ as the finite difference between finite- and zero-field absorption. We have

$$\Delta\alpha(\omega) = \alpha(\omega, F) - \alpha(\omega, 0) \ .$$

The main qualitative features of indirect absorption spectra $\alpha(\omega)$ and differential spectra $\Delta\alpha(\omega)$ result from structure in the absorption strength $|U_{E,F}(0)|^2 S(E)$, and can be easily understood in terms of Eq. (2.1). In Fig. 2 we have plotted the *absorption strength* $|U_{E,F}(0)|^2 S(E)$ and the differential absorption strength $\Delta[|U_{E,F}(0)|^2 S(E)]$ for a barely ionizing field (the reduced field is unity; i.e., $f = 1$, where $f \equiv |e| Fa/R$ and the 1$s$ exciton radius and binding energy are $a$ and $R$, respectively). Four effects on the excitonic absorption strength which are not in the one-electron theory are immediately obvious: (i) The first negative $\delta$ function in the exciton spectrum of $|U_{E,F}(0)|^2 S(E)$ lies lower in energy than the first negative peak in the corresponding one-electron spectrum. As a result of this, the exciton theory predicts a lower energy threshold for the onset of differential absorption strength. (ii) The bound 1$s$ exciton state is responsible for a large negative $\delta$ function in $\Delta[|U_E(0)|^2 S(E)]$. (iii) Significant enhancement is caused by the Coulomb interaction both below $E = 0$ (bound states) and above (continuum states of the exciton). (iv) Exciton theory yields a larger period of spectral oscillation in $\Delta[|U_E(0)|^2 S(E)]$

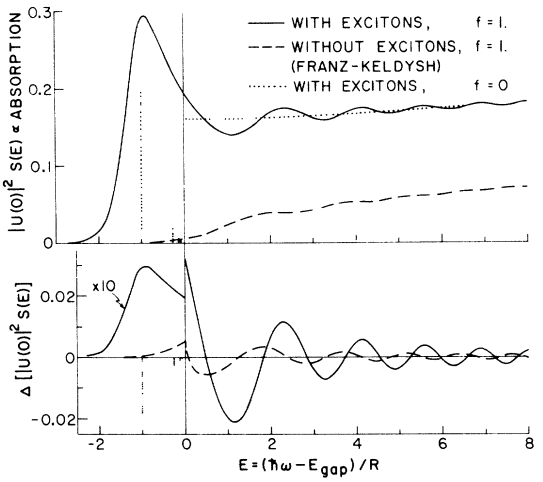


FIG. 2. One-electron and exciton theoretical optical absorption strength and differential absorption strength $\Delta[|U_E(0)|^2 S(E)]$ for a reduced field of $f=1$. The zero-field line without excitons is not plotted, but is a square-root curve about which the Franz-Keldysh curve oscillates. The differential absorption by excitons is not plotted for negative $E$ since it is the difference between $|U_{E,F}(0)|^2 S(E)$ and the sum of $\delta$ functions: $\pi^{-1}\sum_{n=1}^{\infty}(an)^{-3}\delta(E+R/n^2)$. However, the total absorption strength by field-perturbed excitons, scaled down by a factor of 10, is plotted for $E<0$ along with the first few zero-field exciton lines (dotted). Note that the total oscillator strength under the field-perturbed and field-free curves for $E<0$ differ by only a few percent for $f=1$. The excitonic differential absorption for $E<0$ actually joins continuously to that for $E>0$. Recall $f=|e|Fa/R$.

than one-electron theory. (The effect is most obvious if the one-electron theoretical curve is moved to lower energy so that its first positive peak matches up with that of the exciton theory.)

The four exciton effects on the differential absorption strength $\Delta[|U_E(0)|^2 S(E)]$ give rise to the following features in the differential *indirect absorption* spectrum $\Delta\alpha(\omega)$ (see Figs. 3 and 4): (i) The threshold for absorption lies as lower energy. (ii) The bound-exciton $\delta$-function peak is converted to a square root [in contrast with one-electron theory's milder quadratic threshold for $\alpha(\omega, 0)$ (see Fig. 3)] by the convolution Eq. (2.1); thus $\Delta\alpha(\omega)$ has a sudden drop associated with the zero-field exciton on the right-hand side of the first positive peak. (iii) The smoothing process [Eq. (2.1)] preserves the excitonic enhancement in the differential absorption. (iv) The larger period of spectral oscillation of the absorption strength persists after the convolution. These four features of differential indirect absorption spectra are not present in the one-electron Franz-Keldysh theory; but when these exciton effects are added to the one-electron theory, the discrepancies between theory and experiment are removed (as we shall see in Sec. V).

The Coulomb interaction between the electron and the hole is responsible for all four of these qualitative differences from one-electron theory: (i) The attractive Coulomb potential provides lower-energy states for optical absorption, and therefore shifts the absorption threshold to lower energy by approximately one exciton Rydberg ($R$). (ii) The $n$th bound-exciton state in zero field contributes to $\Delta\alpha(\omega)$ an amount

$$-\sum_v \tilde{D}_v(2M_v/\hbar^2)^{3/2}(n^3\pi Ra^3)^{-1}(E_0+R/n^2)^{1/2} . \tag{2.5}$$

This abrupt square-root behavior is to be contrasted with the milder quadratic contribution of free-electron theory:

$$-\sum_v \tilde{D}_v(2M_v/\hbar^2)^{3/2}(32\pi Ra^3)^{-1}(E_0)^2 . \tag{2.6}$$

(iii) The Coulomb interaction attracts the electron to the hole, increasing both the probability $|U(0)|^2$ that they are found together and the absorption strength. (iv) The interaction of the electron with the hole causes the electron to feel that it is in an effective field $F_*$ larger than the applied field $F$—this larger field is responsible for the prolonged period of spectral oscillation. In order

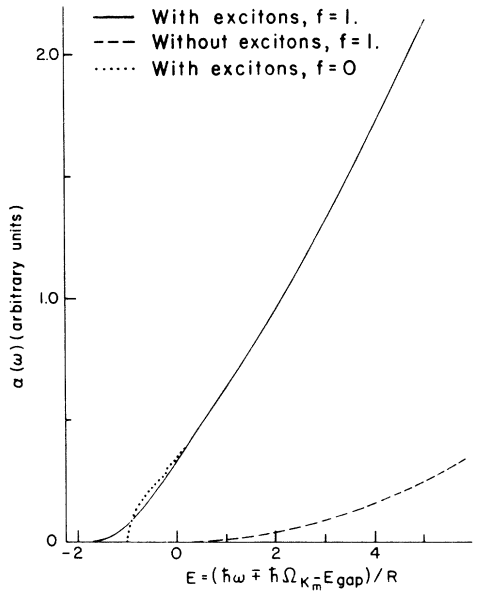


FIG. 3. Absorption coefficient $\alpha(\omega)$ for indirect transitions is plotted for the exciton theory and the one-electron theory (dashed line). The dotted line is $\alpha(\omega)$ for exciton theory with zero applied field; the solid line is for a reduced field of $f=1$. The field-induced difference in $\alpha(\omega)$ for one-electron theory is too small to be shown here. Note the difference in the threshold position and the large enhancement effect due to the Coulombic exciton interaction. The sudden rise above $-\frac{1}{4}$ Rydberg on the zero-field exciton curve is due to the $2s$ exciton bound state.

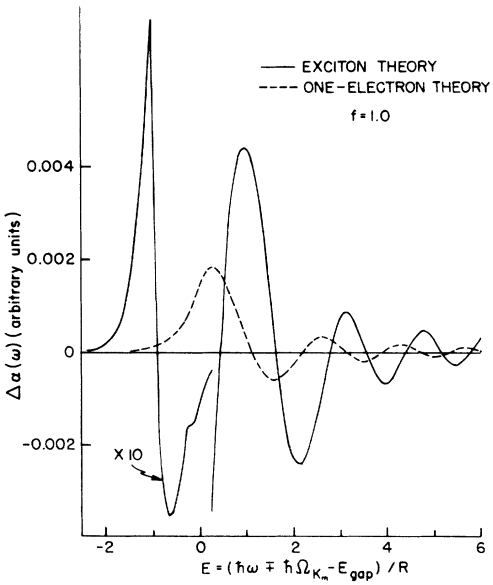


FIG. 4. Differential absorption coefficient for indirect transitions $\Delta\alpha(\omega)$ is plotted here for exciton theory (solid line) and one-electron theory (dashed line). The branch labeled "×10" should be enlarged tenfold so that the discontinuity near $+\frac{1}{4}$ Rydberg actually does not exist. Notice that the exciton theoretical curve, in general, lies lower in energy than the one-electron theoretical curve.

to understand this last argument, we must recall that one-electron theory predicts a period of oscillation which is proportional to $F^{2/3}$; and we note the heuristic argument depicted in Fig. 5, where the electron's wave function emerges from the classically forbidden barrier region and is accelerated to the left-hand side by the applied field and the Coulomb force. As the electron is accelerated toward the hole, it sees an average potential which might be characterized by a larger effective uniform field $F_*$.

In Sec. V we shall see that these qualitative features due to excitons are responsible for the discrepancies between one-electron Franz-Keldysh theory and differential absorption data at the indirect edges of Ge and Si.

## III. FORMALISM

In this section we derive the central expression Eq. (2.1) for the differential optical absorption coefficient $\Delta\alpha(\omega, F)$ using modern techniques and notation, and we make the connection between the present calculation and previous work. Where possible, we adhere to the notation introduced by Ralph[4] and followed in previous papers.[6,12]

The starting points for the calculation of $\Delta\alpha(\omega, F)$ are the expressions relating the absorption coefficient $\alpha(\omega)$ to the imaginary part of the dielectric function $\epsilon_2(\omega)$

$$\alpha(\omega) = [\omega/c\eta(\omega)]\,\epsilon_2(\omega)\,, \tag{3.1}$$

and the linear-response-theory formula for $\epsilon_2(\omega)$ in the dipole approximation[6]

$$\epsilon_2(\omega) = \frac{4\pi}{\omega^2 V}\lim_{\vec{q}\to 0}\left(\sum_i e^{-\beta E_i}\right)^{-1}\sum_{i,f} e^{-\beta E_i} \times |(i|\hat{\epsilon}\cdot\vec{\tilde{J}}(\vec{q})|f)|^2\,\delta(\hbar\omega - E_f + E_i)\,. \tag{3.2}$$

Here $\eta(\omega)$ is the index of refraction for a photon of energy $\hbar\omega$, $c$ is the speed of light, $V$ is the volume of the solid, $\beta = (k_B T)^{-1}$, $k_B$ is Boltzmann's constant, $T$ is the temperature of the solid, $\hat{\epsilon}$ is the unit polarization vector of the absorbed photon, and $\vec{\tilde{J}}(\vec{q})$ is the complex Fourier transform of the current operator.[6] The *exact* initial and final eigenstates of the interacting electron-phonon system, with energies $E_i$ and $E_f$, are $|i)$ and $|f)$, respectively. In order to evaluate $\epsilon_2(\omega)$, we must first determine suitable approximations to the initial and final states.

The Hamiltonian for the interacting electron-phonon system is taken to be

$$H = H_e + H_p + H_{ep} = H_0 + H_{ep}\,, \tag{3.3}$$

where the phonon Hamiltonian is

$$H_p = \sum_{\vec{k},\lambda}^{(1Bz)} \hbar\Omega_{\vec{k}\lambda}\, a^\dagger_{\vec{k}\lambda}\, a_{\vec{k}\lambda}\,, \tag{3.4}$$

the electron Hamiltonian is

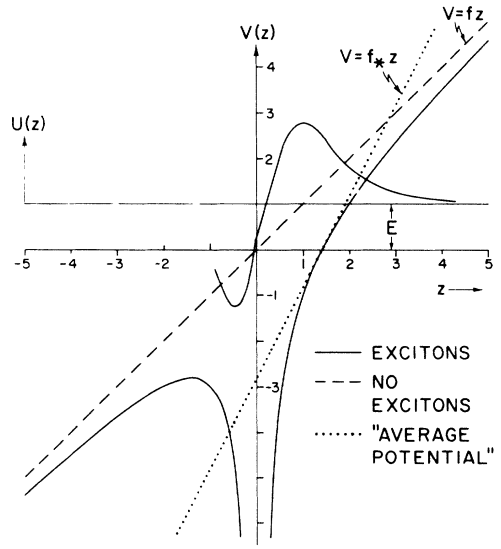


FIG. 5. Wave function $U(z)$ for a continuum state ($E>0$) and potential $V(z)$ along the direction $z$ of the applied field associated with uniform applied field plus electron-hole scattering (i.e., excitons), denoted by solid lines. The "average potential" associated with the larger effective field $f_*$ is denoted by a dotted line. Here $f = |e|Fa/R$ and $f_* = |e|F_* a/R$.

$$H_e = \sum_{n,\vec{k}}^{(1Bz)} \epsilon_n(\vec{k}) c^\dagger_{n\vec{k}} c_{n\vec{k}} \ , \tag{3.5}$$

and the electron-phonon interaction is taken to be linear in the atomic displacement

$$H_{ep} = N^{-1/2} \sum_{\substack{\vec{k},\lambda \\ \vec{q},n,n'}}^{(1Bz)} g(\vec{k},\lambda,n,n')(a^\dagger_{\vec{k}\lambda} - a_{-\vec{k}\lambda}) \times c^\dagger_{n\vec{k}+\vec{q}} c_{n'\vec{q}} + \text{H.c.} \tag{3.6}$$

Here $a^\dagger_{\vec{k}\lambda}$ and $a_{\vec{k}\lambda}$ are boson creation and destruction operators for phonons of energy $\hbar\Omega_{\vec{k}\lambda}$, phonon branch $\lambda$, and wave vector $\vec{k}$; $\epsilon_n(\vec{k})$ is the $n$th energy band; $c^\dagger_{n\vec{k}}$ and $c_{n\vec{k}}$ are fermion creation and destruction operators for an electron in the $n$th energy band $\epsilon_n(\vec{k})$; $g(\vec{k},\lambda,n,n')$ is the electron-phonon coupling; the symbol H.c. means Hermitian conjugate; and (1Bz) over a summation symbol means $\vec{k}$ and $\vec{q}$ are restricted to the first Brillouin zone.

In the initial electronic state all the single-particle electron states in the valence band are filled and the conduction band states are empty; in the indirect absorption final electronic state, there is a hole near the center of the zone and an electron near one of the $\sigma$ equivalent minima $\vec{K}_m (m = 1 \cdots \sigma)$ in the conduction band.[17] The final electronic state has crystal momentum $\vec{K} \simeq \vec{K}_m$ compared with the initial states $\vec{K} \simeq 0$ and the photon's negligible (on the scale of the Brillouin zone) momentum; thus wave-vector conservation forbids the purely electronic transition, and the indirect transition in the perfect crystal is phonon assisted. Thus, to first order in the electron phonon interaction, the initial state is

$$|i\rangle \approx |0\rangle - \sum_{l\neq 0} \frac{|l^0\rangle\langle l^0|H_{ep}|0\rangle}{E^0_l - E^0_i} \ , \tag{3.7}$$

where $|0\rangle$ is the product of the zero-order ground electronic state $|0\rangle\rangle$ times a phonon state $|n_1, n_2, \ldots]$: We have

$$|0\rangle = |0\rangle\rangle |n_1, n_2, \ldots] \ , \tag{3.8}$$

where

$$|n_1, n_2, \ldots] = \prod_{\vec{k},\lambda}^{(1Bz)} \frac{(a^\dagger_{\vec{k},\lambda})^{n_{\vec{k}\lambda}}}{(n_{\vec{k}\lambda})^{1/2}} |0, 0, \ldots] . \tag{3.9}$$

The zero-order initial state energy is

$$E^0_i = \sum_{\vec{k},\lambda}^{(1Bz)} n_{\vec{k}\lambda} \hbar\Omega_{\vec{k}\lambda} . \tag{3.10}$$

If interband ($n \neq n'$) scattering is neglected[18] [i.e., $g(\vec{k},\lambda,n,n') = \delta_{n,n'} g(\vec{k},\lambda,n)$] in the electron-phonon interaction [Eq. (3.6)], the exclusion principle prevents scattering in the filled valence bands. Hence we have

$$\langle l^0|H_{ep}|0\rangle = 0 \tag{3.11}$$

for all $l$ and

$$|i\rangle = |0\rangle . \tag{3.12}$$

The final state has energy

$$E^0_{f\pm} = E^0_i + \hbar\omega \tag{3.13}$$

and, to first order in the electron-phonon interaction, is

$$|f_\pm\rangle \approx |f^0_\pm\rangle - \sum_{l\neq f} \frac{|l^0\rangle\langle l^0|H_{ep}|f^0_\pm\rangle}{E^0_l - E^0_{f\pm}} , \tag{3.14}$$

where $|f^0_\pm\rangle$ is a product of $|f^0\rangle\rangle$ (a superposition of electron-hole pairs) of total wave vector $\vec{K}$ multiplied by a phonon state $|n_1, n_2, \ldots (n_{\mp\vec{K}} \pm 1) \ldots]$, whose wave vector is greater than the ground-state wave vector by $-\vec{K}$. We have

$$|f^0_\pm\rangle = |f^0\rangle\rangle \, |n_1, n_2, \ldots (n_{\mp\vec{K}} \pm 1) \ldots] . \tag{3.15}$$

$|f^0\rangle\rangle$ can be written as[19]

$$|f^0\rangle\rangle = \frac{V}{N} \sum_{\vec{k},\vec{q}}^{(1Bz)} U_\nu(\vec{Q}) \, \Theta_{\vec{K}}(\vec{q} - \vec{k}) \, c^\dagger_{c\vec{q}} \, c_{v\vec{k}} |0\rangle\rangle \ , \tag{3.16}$$

where

$$\vec{Q} = M^{-1}(m_e\vec{k} + m_h\vec{q}) \tag{3.17}$$

is the wave vector for the electron-hole relative motion and $\vec{q} - \vec{k}$ is the wave vector for the center-of-mass motion. (Note that the motion of the hole is time reversed.) Here we have assumed that there are two relevant valence bands $v$ corresponding to light and heavy holes, and one conduction band $c$. The momentum-space wave functions for the center-of-mass and relative motions, respectively, of the exciton are $\Theta_{\vec{K}}(\vec{k})$ and $U_\nu(\vec{k})$, where

$$\Theta_{\vec{K}}(\vec{k}) = N^{-1/2} \textstyle\sum_{\vec{R}^0_n} \Theta_{\vec{K}}(\vec{R}^0_n) \, e^{i\vec{k}\cdot\vec{R}^0_n} , \tag{3.18a}$$

$$U_\nu(\vec{k}) = N^{-1/2} \textstyle\sum_{\vec{R}^0_n} U_\nu(\vec{R}^0_n) \, e^{i\vec{k}\cdot\vec{R}^0_n} . \tag{3.18b}$$

They are normalized such that

$$\sum_{\vec{k}}^{(1Bz)} |\Theta_{\vec{K}}(\vec{k})|^2 = \sum_{\vec{k}}^{(1Bz)} |U_\nu(\vec{k})|^2 = \frac{N}{V} . \tag{3.19}$$

The volume of the crystal is $V$; the quantum numbers labeling the center-of-mass and internal states of the system are $\vec{K}$ and $\nu$, respectively. In the effective-mass approximation, $\Theta_{\vec{K}}(\vec{R}) = V^{-1/2} e^{i\vec{K}\cdot\vec{R}}$, and $U_\nu(\vec{k})$ solves the hydrogenic Schrödinger equation for an exciton in a uniform electric field ($\vec{r}$ and $z$ are operators)

$$\left(\epsilon_c(\vec{k}) - \epsilon_v(\vec{k}) - \frac{e^2}{\epsilon_0 r} - eFz\right) U_\nu(\vec{k}) = E_\nu \, U_\nu(\vec{k}) . \tag{3.20}$$

So the unperturbed final electronic state is

$$|f^0\rangle\rangle = \left(\frac{V}{N}\right)^{1/2} \sum_{\vec{k}}^{(1Bz)} U_\nu\left(\vec{k} + \frac{m_h\vec{K}}{M}\right) c^\dagger_{c\vec{K}+\vec{k}}\, c_{v\vec{k}}\,|0\rangle\rangle . \tag{3.21}$$

Combining Eqs. (3.8), (3.12), and (3.14) we find, to lowest order in the electron-phonon interaction,

$$(i|\hat{\epsilon}\cdot\vec{\tilde{J}}(\vec{q})|f) = -\sum_{l\neq f,0} \frac{\langle 0|\hat{\epsilon}\cdot\vec{\tilde{J}}(\vec{q})|l^0\rangle\langle l^0|H_{ep}|f^0_\pm\rangle}{E^0_l - E^0_{f\pm}} . \tag{3.22}$$

We first expand the intermediate exciton state $|l^0\rangle$, which is similar to $|f_\pm\rangle$ in Eqs. (3.15) and (3.21), and obtain

$$|l^0\rangle = |l^0\rangle\rangle\,|n_1, n_2, \ldots n_{\mp\vec{K}}, \ldots ], \tag{3.23}$$

where

$$|l^0\rangle\rangle = \left(\frac{V}{N}\right)^{1/2} \sum_{\vec{q};\vec{q}}^{(1Bz)} U^l\left(\frac{m_h\vec{q}' + m_e\vec{q}}{M}\right) c^\dagger_{c\vec{q}'}\, c_{v\vec{q}}\,|0\rangle\rangle . \tag{3.24}$$

The current matrix element can be evaluated using the second-quantized representation of the current operator

$$\vec{\tilde{J}}(\vec{q}) = \frac{e}{m}\sum_{\vec{k}} \langle\langle c, \vec{k}+\vec{q}\,|\,\vec{p}\,|\,v, \vec{k}\rangle\rangle\, c^\dagger_{c\vec{k}+\vec{q}}\, c_{v\vec{k}} \tag{3.25}$$

and the exciton states $|l^0\rangle$ to give

$$\lim_{q\to 0}\langle 0|\hat{\epsilon}\cdot\vec{\tilde{J}}(\vec{q})|l^0\rangle = \frac{e}{m}\left(\frac{V}{N}\right)^{1/2}\sum_{\vec{q}'} U^l(\vec{q}')\langle\langle c, \vec{q}'\,|\hat{\epsilon}\cdot\vec{p}\,|v, \vec{q}'\rangle\rangle \equiv \frac{e}{m}\left(\frac{V}{N}\right)^{1/2}\sum_{\vec{q}'} U^l(\vec{q}')\,\hat{\epsilon}\cdot\vec{p}^{\,\vec{q}'}_{cv}(\vec{q}=0). \tag{3.26}$$

Here we have taken the photon wave vector $\vec{q}$, which is negligibly small on the scale of the Brillouin zone, to be zero. To facilitate the sum in Eq. (3.26) we expand the momentum matrix element in powers of $\vec{q}'$ about zero. Since the virtual direct transition to the intermediate state is allowed, we retain only the zeroth-order term in the expansion

$$\vec{p}^{\,\vec{q}'}_{cv}(0) = \vec{p}^{\,0}_{cv}(0) + (\vec{q}'\cdot\nabla_{\vec{q}})\vec{p}^{\,\vec{q}}_{cv}(0)\big|_{\vec{q}=0} + \cdots . \tag{3.27}$$

By the identity

$$\sum_{\vec{q}}^{(1BZ)} U^l(\vec{q}) = N^{1/2}\, U^l(\vec{r}=0) , \tag{3.28}$$

Eq. (3.24) becomes

$$\lim_{\vec{q}\to 0}\langle 0|\hat{\epsilon}\cdot\vec{\tilde{J}}(\vec{q})|l^0\rangle = \frac{e}{m}\, V^{1/2}\hat{\epsilon}\cdot\vec{p}^{\,0}_{cv}(0)\, U^l(\vec{r}=0) . \tag{3.29}$$

The electron-phonon matrix element can be obtained from Eqs. (3.6), (3.15), (3.21), (3.23), and (3.24):

$$\langle l^0|H_{ep}|f^0_\pm\rangle = \frac{V^{1/2}}{N}\sum_{\vec{k},\lambda} U_\nu\left(\vec{k}+\frac{m_h\vec{K}}{M}\right)(n_{\mp\vec{k}}+\tfrac{1}{2}\pm\tfrac{1}{2})^{1/2} \times \frac{V^{1/2}}{N}\,[U^{l*}(\vec{k})g(\vec{K},\lambda,c,c) + U^{l*}(\vec{K}+\vec{k})g(\vec{K},\lambda,v,v)] . \tag{3.30}$$

The transition matrix element in Eq. (3.22) can be written as

$$\lim_{\vec{q}\to 0}(0|\hat{\epsilon}\cdot\vec{\tilde{J}}(\vec{q})|f_\pm) = \frac{e}{m}\left(\frac{V}{N}\right)^{1/2}(n_{\mp\vec{K}}+\tfrac{1}{2}\pm\tfrac{1}{2})^{1/2} \times U_\nu(\vec{r}=0)\,\frac{\hat{\epsilon}\cdot\vec{p}^{\,0}_{cv}(0)G(\vec{K})}{\Delta E^0_\pm} , \tag{3.31}$$

where we used Eq. (3.28) on final state $U_\nu$ and made the assumption that the sum over $l$ depends weakly on $k$ so that

$$\sum_{l,\lambda} VN^{-1/2}U^l(\vec{r}=0)\,\frac{U^{l*}(\vec{k})g(\vec{K},\lambda,c,c) + U^{l*}(\vec{K}+\vec{k})g(\vec{K},\lambda,v,v)}{E^0_{f\pm} - E^0_l} \equiv \frac{G(\vec{K})}{\Delta E^0_\pm} . \tag{3.32}$$

Note that $G(\vec{K}) = \sum_\lambda[g(\vec{K},\lambda,c,c) + g(\vec{K},\lambda,v,v)]$ if the decoupled electron-hole states $\sum_{\vec{q},\vec{q}} c^\dagger_{c\vec{q}'}\, c_{v\vec{q}}|0\rangle\rangle$ were used for the intermediate state $|l^0\rangle\rangle$. The imaginary part of the dielectric function can now be obtained from Eq. (3.2) where the sum over final state $f$ and the $\delta$ function are converted into the operator

$$\frac{\sigma V}{(2\pi)^2}\sum_\nu\left(\frac{2M_\nu}{\hbar^2}\right)^{3/2}\int_{-\infty}^{E_0} dE \times S(E)(\hbar\omega \mp \hbar\Omega_{\vec{K}_m} - E_{gap} - E)^{1/2} \times , \tag{3.33}$$

where $\sigma$ is the total number of equivalent conduction band minima, $M_\nu$ is the sum of the effective masses of the electron averaged over the $\sigma$ minima and the hole of band $v$, $E_0 = \hbar\omega \mp \hbar\Omega_{\vec{K}_m} - E_{gap}$, and $S(E)$ is the final exciton internal density of states. We have also assumed that the phonon dispersion is flat near $\vec{K}_m$. Thus we have

$$\epsilon_2(\omega) = \frac{\sigma e^2 V}{m^2\omega^2 N}\sum_\nu D_\nu\left(\frac{2M_\nu}{\hbar^2}\right)^{3/2}\int_{-\infty}^{E_0} dE$$

$$\times(\hbar\omega \mp \hbar\Omega_{\vec{K}_m} - E_{gap} - E)^{1/2} \times |U_{E,F}(0)|^2 S(E) \quad , \quad (3.34a)$$

where

$$D_v = |\hat{\epsilon}\cdot\vec{p}^{\,0}_{cv}(0)\, G(\vec{K}_m)/\Delta E^0_{\pm}|^2 (n_{\mp\vec{K}_m} + \tfrac{1}{2} \pm \tfrac{1}{2}) \quad . \quad (3.34b)$$

Here we made two of the internal quantum numbers $\nu$ explicit, namely, the exciton energy $E$ and applied field $F$. The change in optical absorption coefficient $\Delta\alpha$ is from Eq. (3.1):

$$\Delta\alpha(\omega) = \sum_v \tilde{D}_v \left(\frac{2M_v}{\hbar^2}\right)^{3/2} \int_{-\infty}^{E_0} dE \times(\hbar\omega \mp \hbar\Omega_{\vec{K}_m} - E_{gap} - E)^{1/2} \times \Delta[|U_E(0)|^2 S(E)] \quad , \quad (3.35a)$$

where

$$\tilde{D}_v = \frac{\sigma e^2 V}{m^2 \omega c \eta(\omega) N} D_v \quad . \quad (3.35b)$$

## IV. NUMERICAL CALCULATION

In this section, we outline the numerical procedures used for calculating the differential electroabsorption coefficient $\Delta\alpha(\omega)$. The starting point of a calculation of $\Delta\alpha(\omega)$ is to evaluate $\Delta[|U_E(0)|^2 \times S(E)]$ in Eqs. (3.35) by solving the relative motion Schrödinger equation with and without an applied electric field $F$:

$$\left(-\frac{\hbar^2}{2\mu}\nabla^2 - \frac{e^2}{\epsilon_0 r} - eFz\right) U_{E,F}(\vec{r}) = E U_{E,F}(\vec{r}) \quad . \quad (4.1)$$

In the absence of the applied field, the hydrogenic equation can be solved analytically to give the well-known Elliott absorption strength as[4]

$$|U_{E,F=0}(0)|^2 S(E) = \sum_{n=1}^{\infty} \frac{\delta(E + R/n^2)}{\pi(an)^3} + \theta(E)[2\pi Ra^3(1 - e^{-2\pi(R/E)^{1/2}})]^{-1} \quad , \quad (4.2a)$$

where $a = \epsilon_0\hbar^2/\mu e^2$ is the first exciton Bohr radius, $R = e^2/2\epsilon_0 a$ is the exciton Rydberg, and $\theta(E)$ is the unit step function. The sum over discrete states in Eq. (4.2a) yields the contributions to the absorption strength by the bound excitons; and the second term is the continuum states' contribution. Note that the two terms join continuously at $E = 0$ at the finite value $1/2\pi Ra^3$. The absorption strength is, in general, larger in value than the familiar $(E/R)^{1/2}(4\pi^2 Ra^3)^{-1}$, which is predicted by one-electron theory in the absence of Coulomb interaction from the evaluation of the density of states alone. This one-electron expression is zero at $E = 0$ and is always less than the exciton result, even at energies far above the band gap, as can be seen by an expansion of the second term of Eq. (4.2a) for large $E$:

$$[2\pi Ra^3(1 - e^{-2\pi(R/E)^{1/2}})]^{-1} = (E/R)^{1/2}(4\pi^2 Ra^3)^{-1} + (4\pi Ra^3)^{-1} + O[(R/E)^{1/2}] \quad . \quad (4.2b)$$

Here $O(x)$ means that terms of order $x$ have been omitted. In addition, we also notice that the bound excitons shift the absorption threshold to lower energy by an amount approximately equal to the Rydberg $R$. As we shall see later, these effects persist also in the presence of an applied electric field.

The only remaining piece of information necessary for obtaining the differential absorption strength $\Delta[|U_E(0)|^2 S(E)]$ is $|U_{E,F}(0)|^2 S(E)$, the absorption strength in finite applied field. The evaluation of $U_{E,F}(0)$ for nonzero $F$ has been discussed in full detail in Sec. I and Ref. 6, where it has been shown that an exact numerical solution of the effective-mass equation (4.1) is required for two reasons. First, perturbation expansions in powers of the electric field strength or in powers of the Coulomb interaction diverge for physically interesting field strengths. Second, since the differential strength $\Delta[|U_E(0)|^2 S(E)]$ is the small difference[20] between the two large numbers $|U_{E,F}(0)|^2 S(E)$ and $|U_{E,0}(0)|^2 S(E)$, any relative error in $|U_{E,F}(0)|^2 S(E)$ will lead to an order-of-magnitude larger relative error in $\Delta[|U_E(0)|^2 S(E)]$. Most approximation schemes are not capable of the accuracy required in order to permit quantitative comparison of theory with experiment. These unfavorable conditions make an intermediate coupling theory desirable. At the current stage of the theory, only direct numerical integration of the Schrödinger equation satisfies such requirements.

Our computation of $\Delta\alpha(\omega)$ was done in two steps: First, the absorption strength $|U_{E,F}(0)|^2 S(E)$ was obtained numerically by solving Eq. (4.1) in the usual fashion.[4-6] Since the exciton system in the applied electric field has no bound states, the absorption strength $|U_{E,F}(0)|^2(E)$ is smooth with broad peaks reminiscent of the $\delta$ functions in Eq. (4.2). Second, $\Delta\alpha(\omega)$ was obtained by numerically convoluting $\Delta[|U_E(0)|^2 S(E)]$, the difference between $|U_{E,F}(0)|^2 S(E)$ and $|U_{E,0}(0)|^2 S(E)$[21] in Eq. (4.2), with the square-root function as in Eqs. (3.35). The convolution must be done with extreme care because a small error on the low-energy side of the absorption strength is greatly amplified by the square root in the convolution (see Fig. 1). To avoid systematic errors in integration, the end of one of the Gaussian quadrature intervals was set at $E = 0$ so as to coincide with the discontinuity of the step function in Eq. (4.2). The sum over $n$ of the $\delta$ functions was done exactly for $n \geq 20$ and the remainder was approximated, to second order in

derivatives with respect to $n$, by means of the Euler-McLaurin summation rule.[22] In order to check the accuracy of the numerical procedures, we simply turned off the Coulomb interaction in our numerical routines and then compared our calculated values of absorption strength and $\Delta\alpha(\omega)$ with the well-known analytic Franz-Keldysh formulas[23]:

$$\Delta[|U_E(0)|^2 S(E)] = \frac{f^{1/3}}{4\pi R a^3}\left(Ai'^{2}(-\zeta) + \zeta Ai^2(-\zeta) - \frac{1}{\pi}\zeta^{1/2}\theta(\zeta)\right) \tag{4.3}$$

and

$$\Delta\alpha(\omega) = \sum_v \tilde{D}_v \left(\frac{2M_v}{\hbar^2}\right)^{3/2} \frac{(\frac{1}{2}f)^{4/3} R^{1/2}}{32\pi a^3}\left\{Ai(-\xi) - \xi Ai'(-\xi) + \xi^2\left[\int_{-\xi}^{\infty} Ai(x)\,dx - \theta(\xi)\right]\right\}, \tag{4.4}$$

where

$$\zeta = \frac{E}{Rf^{2/3}}, \quad \xi = 2^{2/3}\frac{\hbar\omega \mp \hbar\Omega_{\mathbf{K}_m} - E_{\text{gap}}}{Rf^{2/3}}, \tag{4.5}$$

and

$$f = |e|Fa/R .$$

Values of $\Delta[|U_E(0)|^2 S(E)]$ calculated numerically agreed with those evaluated analytically to better than 1%, depending somewhat on the magnitude of the reduced field $f$. The square-root-function convolution procedure was tested by calculating $\Delta\alpha(\omega)$ using Eqs. (3.35) and (4.3) for $\Delta[|U_E(0)|^2 \times S(E)]$. The result thus obtained was checked against the corresponding spectrum gotten from Eq. (4.4); the agreement was better than 1%. These two tests eliminated any large sources of systematic error in the calculation. When computing $\Delta\alpha(\omega)$, with the Coulomb interaction included, we elected to alter by less than 0.1% the absorption strength $|U_{E,F}(0)|^2 S(E)$ obtained by numerically solving the Schrödinger equation (4.1). By doing so, we were able to significantly reduce our computational expenses by merely forcing the final $\Delta\alpha(\omega)$ spectrum to oscillate about zero at photon energies well above threshold. An analysis of this correction scheme[15] showed that the procedure did not alter the shape of the calculated spectrum, its magnitude, or the periods of spectral oscillation; the errors in $\Delta\alpha$ are comparable with the thickness of the plotted line in Fig. 4.

## V. RESULTS AND DISCUSSION

Using the methods discussed in Sec. IV, we have calculated the differential electroabsorption coefficient $\Delta\alpha(\omega)$ for indirect transitions to bound and continuum exciton states in Ge and Si and have compared our calculations with the experimental results presented by Frova, Handler, Germano, and Aspnes.[2] Our results are shown in Fig. 6 for Ge and Fig. 7 for Si. The curves were Lorentzian broadened[24] with $\Gamma = 1.55$ meV for Ge and $\Gamma = 2.0$ meV for Si to achieve best visual fit.[25] These values are to be compared with the experimental resolution of 0.5 meV. The broadening was performed after $\Delta[|U_E(0)|^2 S(E)]$ had been convoluted with a square-root function; the order of performing convolution and broadening is irrelevant. During the fitting procedures we kept the reduced effective mass constant while changing the field strength so as not to affect the exciton Rydberg.[25,26] The reduced effective masses for heavy-hole excitons were taken[2] to be $0.17m_0$ for Si and $0.14m_0$ for Ge, where $m_0$ is the bare electron mass. Transitions due to light holes were neglected because the mass factor $M_v$ in Eqs. (3.35) makes their contribution small.[27] A least-squares fitting attempt, varying the relative sizes of light- and

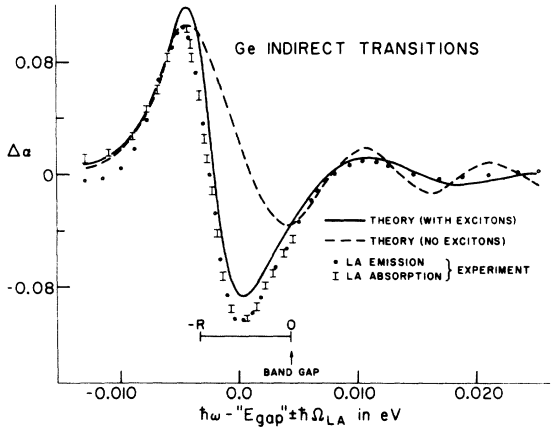


FIG. 6. Differential electroabsorption coefficient $\Delta\alpha$ (in cm$^{-1}$) for indirect transitions in Ge at 296 °K. The abscissa is photon energy minus "$E_{\text{gap}}$" = 0.6657 eV plus or minus the longitudinal acoustical phonon energy (the curves for absorption and emission are superposed). The experimental points (Ref. 2) are denoted by dots (emission) and bars (absorption). The best unbroadened one-electron fit (Ref. 2) is denoted by a dashed line and the present (exciton) theory is denoted by a solid line. The present theory obtains $f = 0.872$, $E_{\text{gap}} = 0.6701$ eV, and $\Gamma = 1.55$ meV in contrast to the values $f = 0.744$ and $E_{\text{gap}} = 0.6595$ eV of the one-electron theory.

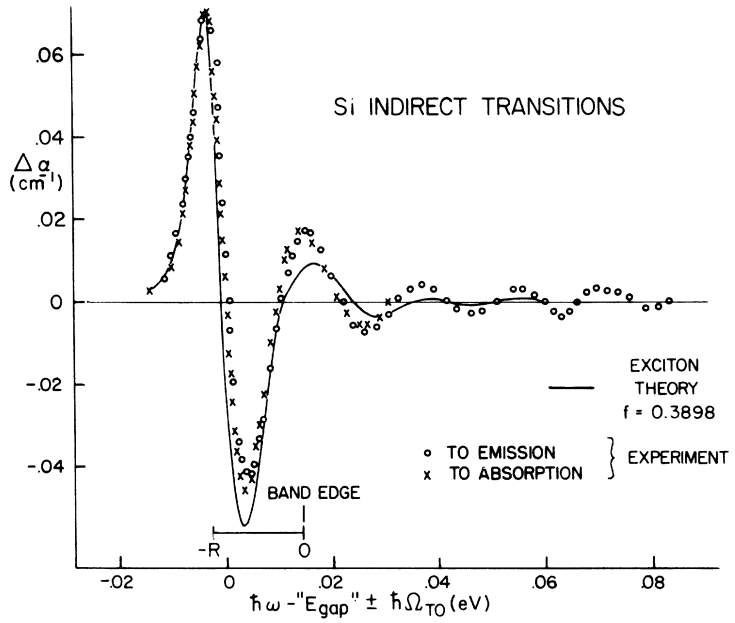


FIG. 7. Differential electroabsorption coefficient $\Delta\alpha$(in $cm^{-1}$) for indirect transitions in Si at 296 °K. The abscissa is photon energy minus "$E_{gap}$" = 1.1117 eV plus or minus the transverse optical phonon energy (the curve for absorption and emission are superposed). The experimental points are denoted by circles (emission) and crosses (absorption). The fit of exciton theory is denoted by a solid line. The present theory obtains $f = 0.3898$, $E_{gap} = 1.1260$ eV, and $\Gamma = 2.0$ meV. The effective reduced mass was taken from Ref. 2 to be $0.17m_0$ with an applied field $F = 1.808 \times 10^4$ V/cm.

heavy-hole contributions, showed that the light hole in Si accounted for less than 5% of the $\Delta\alpha(\omega)$ spectrum. The final fitted values for the fields $F$ were $1.114 \times 10^4$ and $1.808 \times 10^4$ V/cm as compared with the experimental values of $0.95 \times 10^4$ and $1.4 \times 10^4$ V/cm for Ge and Si, respectively.

By comparing the one-electron and exciton theoretical fits to experimental data in Figs. 6–8 we notice that the exciton fits are superior in four respects: (i) The exciton theory predicts a larger band gap than one-electron theory. In order to get agreement with experiment, one-electron theory has to artificially shift the indirect gaps to energies lower than "$E_{gap}$" by 6.2 meV in Ge and 5.7 meV in Si (as compared with exciton binding energies of 7.64 and 16.896 meV). The discrepancy between one-electron theory and experiment is even greater (10.5 and 23.1 meV), as we shall show, because the values of "$E_{gap}$" seem to be unrealistically smaller than the actual band-gap

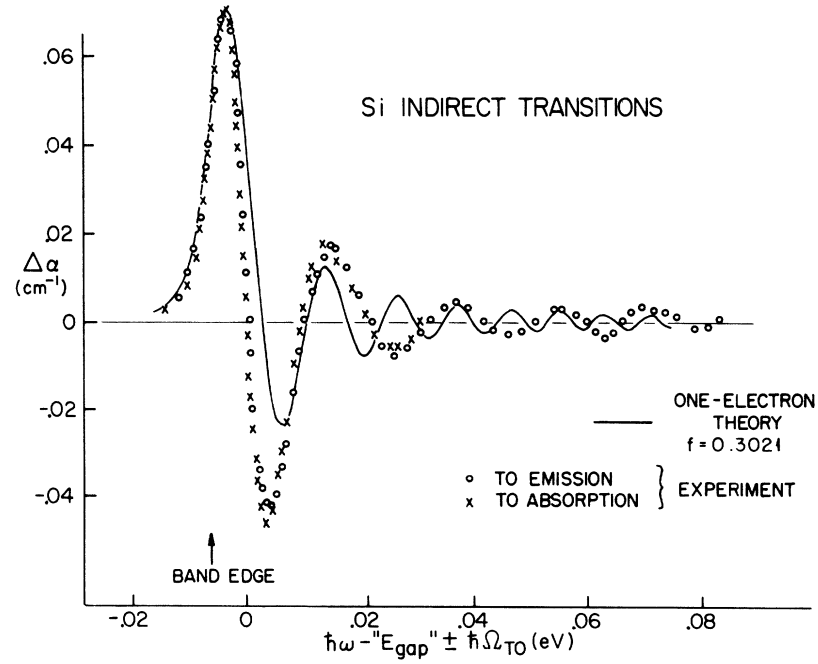


FIG. 8. Differential electroabsorption coefficient in Si at 296 °K. The solid line denotes the fit of one-electron theory with $f = 0.3021$, or, equivalently, for the measured field of $F = 1.4 \times 10^4$ V/cm and a fitted effective reduced mass $\mu = 0.18m_0$.

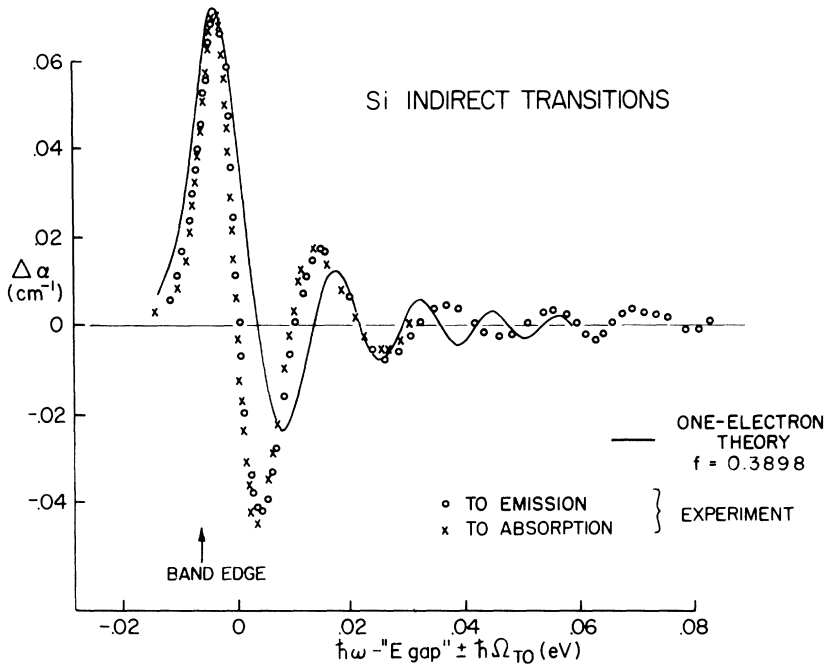


FIG. 9. Differential electroabsorption coefficient in Si at 296 °K. The solid line denotes the fit with one-electron theory at $f = 0.3898$ or, equivalently, $F = 1.808 \times 10^4$ V/cm, which is used for the fit with exciton theory in Fig. 7.

energies. (ii) Exciton theory reproduces the abrupt decrease of $\Delta\alpha(\omega)$ immediately after the first positive peak in each spectrum. (iii) The matrix element necessary to obtain an accurate fit to the first peak of each spectrum is smaller for exciton theory than for one-electron (0.588$\hbar$/Å and 0.158$\hbar$/Å vs 0.187$\hbar$/Å and 0.334$\hbar$/Å for Si and Ge, respectively) theory—hence bound and continuum excitons enhance the differential spectra. (iv) Exciton theory predicts a longer and more accurate period of oscillation for $\Delta\alpha(\omega)$. The value of reduced field $f$ used in the exciton fits is somewhat larger than $f$ used in the one-electron fits; however, this increase in $f$ accounts for only a fraction of the increased period (as may be seen by comparing Figs. 7–9). These qualitative changes in the theoretical spectra brought about by the final-state Coulomb interaction between the electron and the hole are just those exciton effects discussed in Sec. II.

These four qualitative exciton-related features of indirect differential absorption spectra lead to a few useful rules of thumb for fitting experimental spectra: (i) The sharp drop in $\Delta\alpha(\omega)$ after the first peak is due to the 1$s$ exciton and, therefore, the indirect band gap lies approximately (due to broadening)[28] one exciton Rydberg above the drop. (ii) The 2$s$ exciton state lies between the indirect gap and the 1$s$ exciton, giving a contribution of

$$\sum_v \tilde{D}_v \left(\frac{2M_v}{\hbar^2}\right)^{3/2} (\hbar\omega \mp \hbar\Omega_{\vec{K}_m} - E_{\text{gap}} + \tfrac{1}{4}R)^{1/2}$$

to $\Delta\alpha(\omega)$; in the Si data (Fig. 7) there is a barely visible decrease in slope of $\Delta\alpha(\omega)$ at an energy $\frac{1}{4}R$ below the band edge[29]; this change in $\Delta\alpha(\omega)$ may be due to the 2$s$ exciton. (iii) For zero broadening ($\Gamma = 0$), the contribution of the 1$s$ exciton to $\Delta\alpha(\omega)$ is responsible for an *abrupt* square-root drop on the high-energy side of the first peak; thus, the nonabruptness of this drop in experimental spectra gives a rough measure of the size of $\Gamma$.

In addition to the qualitative information contained in differential absorption data, there is considerable quantitative information. Perhaps the easiest and most reliable quantity which can be extracted from a spectrum is the energy $E_{\text{gap}}$ of the indirect band gap, which is one of the parameters of the fitting procedure. In the case of Si and Ge, the values of $E_{\text{gap}} - R$ are well known from the work of MacFarlane, McLean, Quarrington, and Roberts,[11] whose data can be extrapolated quadratically to a temperature of 296 °K. In Table I the values $E_{\text{gap}}$, extracted from the data of MacFarlane *et al.*, are compared with the numbers for $E_{\text{gap}}$ obtained by the exciton fit (present work) and the one-electron fit[2] to the electroabsorption data; values of the heavy-hole exciton binding energies, reduced masses, and static dielectric constants are also listed in Table I. Note that the excition fit produced values of $E_{\text{gap}}$ in very good agreement with the independently measured values.

A second quantity which can be extracted in principle from the fit of theory to data is the matrix element which determines the strength of the indirect transition. However, the interplay between thermal broadening parameter $\Gamma$ and the transition strength makes it difficult for the fitting procedure

TABLE I. Values of the indirect band-gap energies $E_{gap}$, heavy-hole exciton Rydbergs $R$, heavy-hole exciton reduced masses $\mu$, and the static dielectric constants $\epsilon_0$.

| | $E_{gap}$ (in eV) | | | | | | |
|---|---|---|---|---|---|---|---|
| Substance | Measured[a] | Exciton theory[b] | One-electron theory[c] | "$E_{gap}$"[d] | $R$[e] (eV) | $\mu/m_0$[f] | $\epsilon_0$[g] |
| Ge | 0.6700 | 0.6701 | 0.6595 | 0.6657 | 0.00764 | 0.14 | 15.8 |
| Si | 1.1291 | 1.1260 | 1.1060 | 1.1117 | 0.01689 | 0.17 | 11.7 |

[a]Quadratically extrapolated from the data for $E_{gap}-R$ taken by MacFarlane *et al.* (Ref. 11), using a heavy-hole Rydberg $R$.

[b]Present work, values extracted from fit to electroabsorption experiment (Ref. 2).

[c]Reference 2, values extracted from fit to electroabsorption data (Ref. 2).

[d]Values of $E_{gap}$ used in Ref. 2.

[e]$R = 13.605\,\mathrm{eV}\,\mu/\epsilon_0^2$.

[f]Reference 2.

[g]Reference 30.

to determine the value of the transition matrix element precisely, for an increase in $\Gamma$ reduces the heights of the differential absorption peaks in a manner which can be compensated for by increasing the matrix element. Thus, at present, the largest impediment to an extremely precise theory seems to be the absence of an accurate independent determination of the energy-dependent broadening. In spite of these difficulties, we have extracted estimates of the effective momentum matrix elements $\vec{p} = \hat{\epsilon} \cdot \vec{p}_{cv}^{0}(0) G(\vec{K}_m)/\Delta E$ from the theoretical fits, and have obtained values of $0.0588\hbar/\text{Å}$ and $0.158\hbar/\text{Å}$ for Si and Ge, respectively.

Finally, the exciton reduced mass can be extracted from the theoretical fit if the applied field $F$ is both spatially uniform and accurately known, and if the broadening function $\Gamma$ is known as a function of energy. Uncertainties concerning the value of $\Gamma$ and its variation with energy led us to use the cyclotron-resonance masses as input for our calculations. However, based on our experience with Si and Ge, we believe the theory of excitonic electroabsorption may now be sufficiently advanced so that only the problem of determining the broadening function $\Gamma$ prevents the accurate determination by electromodulation experiments of effective masses, band gaps, matrix elements, and energy band structure, in general.

Thus far we have found that the exciton theory explains the major discrepancies between one-electron theory and experiment, and that it provides access to quantitative information about energy gaps, matrix elements, effective masses, and electron-phonon interactions. However, the present work fails to accurately fit the amplitudes of high-energy oscillations of the Si electroabsorption data. Furthermore, the present work succeeds in fitting data at the indirect edges of Si and Ge, even though calculations of direct electroabsorption in these materials found significant discrepancies between theory and experiment which were ascribed to nonuniform electric fields.[31]

The failure of the present work to adequately describe the high-energy oscillations in Si is probably due to two effects: (i) The experiment, as performed, does not measure the finite difference between absorption coefficients at finite field and zero field, but instead it measures a quantity closer to the derivative of the absorption coefficient at a finite field.[32] (ii) To a lesser extent, the disagreement between theory and experiment can be partially remedied by increasing the theoretical broadening $\Gamma$ and the transition matrix element, thereby increasing the amplitude of the high-energy oscillations relative to $\Delta\alpha(\omega)$ near the bound-exciton spectral region.

The fact that the present calculation of the indirect differential absorption coefficient in Ge yields excellent agreement with experiment while previous calculations of direct transitions in Ge failed to achieve agreement with similar experiments can be explained by the following two considerations. (i) The square-root convolution [Eqs. (3.35)] is a smoothing process which may tend to average out some of the effects of nonuniform fields. (ii) The absorption coefficient at the indirect edge of Ge ($\sim 4\ \mathrm{cm}^{-1}$) is about 20 times weaker than the absorption coefficient at the direct edge ($\sim 100\ \mathrm{cm}^{-1}$). Thus the absorption occurs in the bulk of the sample and surface effects which lead to nonuniformities in the applied electric field are less important in indirect transitions.

## VI. CONCLUSIONS

Calculations of the differential electroabsorption coefficient for indirect optical transitions reveal that excitons are responsible for qualitative features in experimental spectra which were not accounted for by one-electron theory. In addition, the fits of exciton theory to experimental data for Ge and Si yield quantitative information about energy gaps, matrix elements, and effective masses.

At present, the greatest impediment to the development of the theory of electroabsorption seems to be a lack of a quantitative *a priori* knowledge of broadening mechanisms; thus, future theoretical

effort should concentrate on the effects of broadening processes and inhomogeneous fields[31] on electromodulation spectra. Once those effects are quantitatively understood, extensive calculations of the sort described here promise to expose many of the secrets of band structure hidden in electroabsorption spectra. Thus electromodulation spectra may eventually yield valuable quantitative information about the effects of electron-electron and electron-phonon interactions on optical spectra.

## APPENDIX: DERIVATIVES OF $\alpha(\omega,F)$

In one-electron theory for zero applied field, $|U_{E,0}(0)|^2$ is a constant (the relative-motion envelope function is a plane wave) and the density of states is proportional to

$$|U_{E,0}(0)|^2 S(E) = \frac{(E/R)^{1/2}}{4\pi^2 R a^3} \ . \tag{A1}$$

The square-root dependence of the absorption strength gives an indirect zero-field absorption coefficient via Eq. (2.4) which is quadratic in $\hbar\omega$:

$$\alpha(\omega,0) = \sum_v \tilde{D}_v \left(\frac{2M_v}{\hbar^2}\right)^{3/2} (32\pi R^{3/2} a^3)^{-1} \times (\hbar\omega \mp \hbar\Omega_{\vec{K}_m} - E_{\rm gap})^2 \tag{A2}$$

and

$$\frac{\delta\alpha(\omega,0)}{\delta\hbar\omega} = \sum_v \tilde{D}_v \left(\frac{2M_v}{\hbar^2}\right)^{3/2} (16\pi R^{3/2} a^3)^{-1} \times (\hbar\omega \mp \hbar\Omega_{\vec{K}_m} - E_{\rm gap}) \ . \tag{A3}$$

In a finite field $F$, Franz-Keldysh theory gives[3,23]

$$|U_{E,F}(0)|^2 S(E) = (f^{1/3}/4\pi R a^3)[Ai'^2(-\zeta) + \zeta Ai^2(-\zeta)] \tag{A4a}$$

$$= (4\pi R^{3/2} a^3)^{-1} \theta(E) E^{1/2} [1 - (2\zeta^{3/2})^{-1} SC + (48\zeta^3)^{-1}(10 - 17S^2) + O(\zeta^{-9/2})] + (16\pi^2 R^{3/2} a^3)^{-1} \theta(-E) |E|^{1/2} e^{-4|\zeta|^{3/2}/3} \times [(2|\zeta|^{3/2})^{-1} - 17/(48|\zeta|^3) + O(|\zeta|^{-9/2})] \ . \tag{A4b}$$

Here we have

$$\zeta = E/(Rf^{2/3}) \ , \tag{A5a}$$

$$f = |e| Fa/R \ , \tag{A5b}$$

$$C = \cos(\tfrac{2}{3}\zeta^{3/2} + \tfrac{1}{4}\pi) \ , \tag{A5c}$$

and

$$S = \sin(\tfrac{2}{3}\zeta^{3/2} + \tfrac{1}{4}\pi) \ . \tag{A5d}$$

The unit step function is $\theta(E)$, and $O(x)$ means that terms of order $x$ have been omitted.

The one-electron indirect absorption coefficient has been given by Aspnes,[23]

$$\alpha(\omega,F) = \sum_v \tilde{D}_v \left(\frac{2M_v}{\hbar^2}\right)^{3/2} (32\pi a^3)^{-1} (\tfrac{1}{2}f)^{4/3} R^{1/2} \left(Ai(-\xi) - \xi Ai'(-\xi) + \xi^2 \int_{-\xi}^{\infty} Ai(x)\,dx\right) \tag{A6a}$$

$$= \sum_v \tilde{D}_v \left(\frac{2M_v}{\hbar^2}\right)^{3/2} (32\pi R^{3/2} a^3)^{-1} E_0^2 \left[\theta(E_0)\left(1 + \frac{41}{48\pi^{1/2}}\,\xi^{-9/4} \sin(\tfrac{2}{3}\xi^{3/2} + \tfrac{1}{4}\pi) - \frac{25}{4608\pi^{1/2}}\,\xi^{-3/4} \cos(\tfrac{2}{3}\xi^{3/2} + \tfrac{1}{4}\pi)\right) + \theta(-E_0)\, e^{-2|\zeta|^{3/2}/3}\left(\frac{41}{96\pi^{1/2}}\,|\xi|^{-9/4} - \frac{25}{9216\pi^{1/2}}\,|\xi|^{-15/4}\right) + O(|\xi|^{-21/4})\right]. \tag{A6b}$$

Here $\xi = E_0/[R(f/2)^{2/3}]$ and $E_0 = \hbar\omega \mp \hbar\Omega_{\vec{K}_m} - E_{\rm gap}$. Thus, just below the absorption threshold, one-electron theory predicts

$$\frac{\delta\alpha(\omega,F)}{\delta F} = \sum_v \tilde{D}_v \left(\frac{2M_v}{\hbar^2}\right)^{3/2} [96\pi R^{3/2} (\tfrac{1}{2}f)^{1/3}]^{-1} |e| E_0\, e^{-2|\zeta|^{3/2}/3} \times \left(\frac{41}{96\pi^{1/2}} (\tfrac{9}{4}|\xi|^{-5/4} + |\xi|^{1/4}) - \frac{25}{9216\pi^{1/2}} (\tfrac{15}{4}|\xi|^{-11/4} + |\xi|^{-5/4})\right). \tag{A7}$$

In exciton theory, the corresponding quantities near the absorption threshold are

$$|U_{E,0}(0)|^2 S(E) = (\pi a^3)^{-1} \delta(E + R) \ , \tag{A8}$$

$$\alpha(\omega,0) = \sum_v \tilde{D}_v \left(\frac{2M_v}{\hbar^2}\right)^{3/2} (\pi a^3)^{-1} (E_0 + R)^{1/2} \ , \tag{A9}$$

$$\frac{\delta\alpha(\omega,0)}{\delta\hbar\omega} = \sum_v \tilde{D}_v \left(\frac{2M_v}{\hbar^2}\right)^{3/2} (2\pi a^3)^{-1} (E_0 + R)^{-1/2} \ , \tag{A10}$$

$$|U_{E,F}(0)|^2 S(E) = (\pi a^3)^{-1} \delta(E + R + \tfrac{9}{8} f^2 R) \ , \tag{A11}$$

$$\alpha(\omega,F) = \sum_v \tilde{D}_v \left(\frac{2M_v}{\hbar^2}\right)^{3/2} (\pi a^3)^{-1} (E_0 + R + \tfrac{9}{8} f^2 R)^{1/2} \ , \tag{A12}$$

$$\frac{\delta\alpha(\omega, F)}{\delta F} = \sum_{v} \tilde{D}_v \left(\frac{2M_v}{\hbar^2}\right)^{3/2} \left(\frac{9|e|f}{8\pi a^2}\right) (E_0 + R + \tfrac{9}{8} f^2 R)^{-1/2} . \tag{A13}$$

Thus, excitons completely modified the one-electron shape of the derivatives of $\alpha(\omega, F)$ and alter the indirect differential electroabsorption $\Delta\alpha(\omega)$, which for small fields $F$ is

$$\Delta\alpha(\omega) = \frac{\delta\alpha}{\delta F} F + \cdots .$$

---

†Work supported by the Air Force Office of Scientific Research under Contract No. AF 49(638)1545.

*Present address: Department of Physics and Astronomy, University of Maryland, College Park, Md. 20742.

‡National Science Foundation Fellow. Present address: Cavendish Laboratory, Free School Lane, Cambridge, England.

[1]B. O. Seraphin, in *Semiconductors and Semimetals*, edited by R. K. Willardson and A. Beer (Academic, New York, 1970), Vol. VI; M. Cardona, in *Modulation Spectroscopy*, Suppl. II of *Solid State Physics*, edited by F. Seitz, D. Turnbull, and H. Ehrenreich (Academic, New York, 1969).

[2]A. Frova, P. Handler, F. A. Germano, and D. E. Aspnes, Phys. Rev. 145, 575 (1966).

[3]C. M. Penchina, Phys. Rev. 138, A924 (1965); M. Chester and L. Fritsche, *ibid.* 139, A518 (1965); for an up-to-date review, see D. E. Aspnes and N. Bottka, in *Semiconductors and Semimetals*, edited by R. K. Willardson and A. Beer (Academic, New York, 1970), Vol. VI.

[4]H. I. Ralph, J. Phys. C 1, 378 (1968); D. F. Blossey, Bull. Am. Phys. Soc. 14, 429 (1969); Phys. Rev. B 3, 1382 (1971).

[5]C. B. Duke, Phys. Rev. Letters 15, 625 (1965); C. B. Duke and M. E. Alferieff, Phys. Rev. 145, 583 (1966).

[6]J. D. Dow and D. Redfield, Phys. Rev. B 1, 3358 (1970).

[7]Preliminary results have been reported previously in B. Y. Lao, J. D. Dow, and F. C. Weinstein, Phys. Rev. Letters 26, 499 (1971).

[8]R. J. Elliott, Phys. Rev. 108, 1384 (1957).

[9]G. Dresselhaus, A. F. Kip, and C. Kittel, Phys. Rev. 98, 368 (1954); M. Cardona and F. H. Pollak, *ibid.* 142, 530 (1966); D. Long, *Energy Bands in Semiconductors* (Interscience, New York, 1968).

[10]T. P. McLean, in *Progress in Semiconductors*, edited by A. F. Gibson (Heywood, London, 1960), Vol. 5, p. 53; M. D. Sturge, Phys. Rev. 127, 768 (1962).

[11]G. G. MacFarlane, T. P. McLean, J. E. Quarrington, and V. Roberts, Phys. Rev. 108, 1377 (1957); 111, 1245 (1958).

[12]J. D. Dow, B. Y. Lao, and S. A. Newman, Phys. Rev. B 3, 2571 (1971).

[13]F. C. Weinstein, J. D. Dow, and B. Y. Lao, Phys. Status Solidi 43, K105 (1971); Phys. Rev. B 4, 3502 (1971).

[14]Note that here $E$ has the units of energy, in contrast with the unitless $E \equiv (\hbar\omega - E_{gap})/R$ used in Refs. 6 and 12 ($R$ is the 1$s$ exciton binding energy).

[15]B. Y. Lao, Ph.D. thesis (Princeton University, 1971) (unpublished).

[16]The relevant "largeness" parameter is $f = |e|F\, a/R$, the field-induced potential energy drop across the radius $a$ of the 1$s$ exciton divided by the exciton binding energy $R$. Qualitatively, for $f > 1$, the exciton is ionized.

[17]Near the conduction band minima in Ge there are four identical energy ellipsoids along the [111] direction at the zone boundary. In Si there are six ellipsoids along the [100] direction. Thus an electric field applied in the (111) direction, as in the experiments of Ref. 2, will leave all the ellipsoids in Si equivalent, but in Ge, one ellipsoid will be different from the other three. We neglect this inequivalence, which should lead to quite small corrections.

[18]Assume the phonon interacts with the electron via the electrostatic potential $e\vec{F}\cdot\vec{r}\, e^{i\vec{k}\cdot\vec{r}}$, then the interband coupling to first order is smaller than intraband coupling by a factor of $(a_L/a)^2$ for $k < 1/a$ or $a_L/a$ for $k > 1/a$, where $a_L$ is the lattice constant and $a$ is the exciton Bohr radius.

[19]This differs from Eq. (3.12) of Ref. 6 only in a phase factor, thus we have

$$|f^0\rangle\rangle = V^{1/2} N^{-1} \sum_{\vec{r},\vec{R}} U_v(\vec{r}) e^{i\vec{K}\cdot\vec{R}} c^{\dagger}_{c\vec{R}_e} c_{v\vec{R}_h} |0\rangle\rangle,$$

where $\vec{r} = \vec{R}_e - \vec{R}_h$ is the relative position vector and $\vec{R} = (m_e\vec{R}_e + m_h\vec{R}_h)/M$ is the center-of-mass position vector. Defining

$$c_{n\vec{R}} = N^{-1/2} \sum_{\vec{k}}^{(\mathrm{B.z.})} e^{-i\vec{k}\cdot\vec{R}} c_{n\vec{k}},$$

Eq. (3.16) then immediately follows.

[20]$\Delta[|U_E(0)|^2 S(E)]$ is typically less than 10% of $|U_E(0)|^2 \times S(E)$.

[21]For $E_0$ positive and $F = 0$, we have found a rational approximation to

$$f(E_0) = \sum_{n=1}^{\infty} n^{-3}\pi^{-1}(E_0 + n^{-2})^{1/2} + (2\pi)^{-1} \int_0^{E_0} (E_0 - E) \times (1 - e^{-2\pi E^{-1/2}})^{-1} dE.$$

It is

$$f(x^2) = \frac{\pi^3}{90} + \frac{x^4}{32\pi} + \frac{a_1 x + a_2 x^2 + a_3 x^3 + a_4 x^4}{1 + a_5 x}$$

where, for $x^2 \lesssim 10$, the $a$'s are 0.0106101, 0.234949, 0.283353, 0.0044413, and 0.0254727, and the error is less than 0.002. For $x^2 \gtrsim 50$, the $a$'s are 0.511313, 0.174432, 0.147264, 0.0358471, and 0.677758, and the error is less than 0.2%. For $10 \lesssim x^2 \lesssim 50$, the $a$'s are 0.0538592, 0.192541, 0.0777258, 0.0107118, and 0.201189, and the error is less than 0.2%.

[22]M. Abramowitz and I. A. Stegun, *Handbook of Mathematical Functions* (Dover, New York, 1965), p. 16.

[23]D. E. Aspnes, Phys. Rev. 147, 554 (1966); 153, 972 (1967).

[24]The Lorentzian broadened differential absorption $\Delta\alpha(\omega, 0)$ by

$$\Delta\alpha(\omega, \Gamma) = \int_{-\infty}^{\infty} L(\omega - \omega', \Gamma)\Delta\alpha(\omega', 0) d\omega',$$

where $L(\omega, \Gamma) = (\Gamma/\pi\hbar)\ (\omega^2 + \Gamma^2/\hbar^2)^{-1}$.

[25]We did not obtain a least-squares fit varying the effective mass and broadening parameter for the following reasons: (i) Our computer budget was quite limited [we

could only afford to calculate $\Delta\alpha(\omega)$ three times]; (ii) our main interest was in explaining the principal physical features of the spectra which are caused by excitons; (iii) an extremely precise fit to the data requires a knowledge of the effects of nonuniform fields, energy-dependent broadening, and bandwarping—to some extent these effects afford the fitting procedure with additional parameters for optimizing the agreement between experiment and theory without any confidence that these optimal values of the fitting parameters are physically realistic. For example, in our fit with the Si data (Fig. 7), we could increase the agreement on the high-energy side of the spectrum by reducing the value of $\Gamma$ by about 50%. This would cause the theoretical curve to be too large in the bound-exciton region, a situation which could be fixed by judiciously altering the transition matrix element, the reduced effective mass, and the field inhomogeneity. However, such a procedure tends to obscure the underlying physics and should be avoided; furthermore, we believe that there is a physical reason for the discrepancy between theory and experiment at high energy. This discrepancy will be discussed later in Sec. V.

[26]Note that we have $f = |e|Fa/R \propto \mu^{-2}$ and $R \propto \mu$. The fitting procedure determines $f$ and $R$, but only approximately, so that variation of $f$ may be ascribed to variation of $F$ or $m$ or both.

[27]In Ge, the light and heavy holes have masses of $0.04\,m_0$ and $0.3m_0$, respectively. [See C. Kittel, *Introduction to Solid State Physics*, 3rd ed. (Wiley, New York, 1966), p. 322.] The average conduction band mass is $0.263m_0$. Thus the total masses and the reduced masses are $0.3m_0$ and $0.035m_0$ for the light-hole band and $0.563m_0$ and $0.14m_0$ for the heavy-hole band. The corresponding numbers (Ref. 2) for Si are $0.16m_0$, $0.49m_0$, $0.26m_0$, $0.42\,m_0$, $0.10m_0$, $0.75m_0$, and $0.17m_0$, respectively. Near $E=0$, the indirect absorption coefficient varies nearly as $\mu^2M^{3/2}$. Thus we have $[\mu^2M^{3/2}\ (\text{light})]/[\mu^2M^{3/2}\ (\text{heavy})]$ equal to 0.024 and 0.15.

[28]The high-energy side of the first peak of $\Delta\alpha(\omega)$ is steeper than the low-energy side. Thus, when the peak is broadened, it generally moves to lower energy.

[29]An additional differentiation of $\Delta\alpha(\omega)$ (with respect to, say, photon wavelength) would probably exhibit the broadened $2s$ state dramatically.

[30]D. Long, *Energy Bands in Semiconductors* (Wiley, New York, 1968), p. 163.

[31]D. E. Aspnes and A. Frova, Solid State Commun. 7, 155 (1969).

[32]This can be seen by noting that $\Delta\alpha(\omega, F)$ for energies well above $E_{\text{gap}}$ is (in the one-electron approximation) from the Appendix

$$\Delta\alpha(\omega) = \tilde{D}_v\left(\frac{2M_v}{\hbar^2}\right)^{3/2}(32\pi a^3R^{3/2})^{-1}E_0^2[A\xi^{-9/4}\sin(\tfrac{2}{3}\xi^{3/2}+\tfrac{1}{4}\pi) - B\xi^{-15/4}\cos(\tfrac{2}{3}\xi^{3/2}+\tfrac{1}{4}\pi)+O(\xi^{-21/4})],$$

where $A$ and $B$ are constants, $\xi = E_0/[R(\frac{1}{2}f)^{2/3}]$, and $E_0 = \hbar\omega \mp \hbar\Omega_{\vec{K}m} - E_{\text{gap}}$. In contrast, the derivative is

$$F\frac{\partial}{\partial F}\alpha(\omega, F) = \tfrac{3}{2}\Delta\alpha(\omega) - \tilde{D}_v\left(\frac{2M}{\hbar^2}\right)^{3/2}(32\pi a^3R^{3/2})^{-1}E_0^2 \times[(\tfrac{2}{3}A\xi^{-3/4}+B\xi^{-15/4})\cos(\tfrac{2}{3}\xi^{3/2}+\tfrac{1}{4}\pi) + \tfrac{2}{3}B\xi^{-9/4}\sin(\tfrac{2}{3}\xi^{3/2}+\tfrac{1}{4}\pi)].$$

Note that for high energies the term with $\xi^{-3/4}$ is larger than the dominant term in $\Delta\alpha(\omega, F)$ which only goes as $\xi^{-9/4}$.

PHYSICAL REVIEW B VOLUME 4, NUMBER 12 15 DECEMBER 1971

# Electron-Tunneling Studies of a Quantized Surface Accumulation Layer

D. C. Tsui
*Bell Telephone Laboratories, Murray Hill, New Jersey* 07974
(Received 22 July 1971)

This paper describes an experiment on electron tunneling through $n$-type InAs-oxide-Pb junctions and discusses in detail two results which are pertinent to the quantization of an accumulation layer at the InAs surface. First, the tunneling curves $dI/dV$ vs $V$ and $d^2I/dV^2$ vs $V$ show structures reflecting the energy minima of two-dimensional electric subbands. The bias position of these structures gives a direct measure of the energy of the quantized levels. Second, when a quantizing magnetic field is applied perpendicular to the junction surface, oscillations are observed in the tunneling curves. These oscillations reflect the Landau-level spectra of electrons in the electric subbands. They give a direct measure of the effective mass of the surface electrons.

## I. INTRODUCTION

In an accumulation or inversion layer of a semiconductor surface, if the electric field associated with the surface layer is sufficiently strong, the energy due to a carrier's motion normal to the surface is quantized into discrete levels. Since a continuum of energy is allowed for motion parallel to the surface, the energy structure of the surface carrier is a series of two-dimensional bands called electric subbands, each corresponding to a quantized level. The existence of these two-dimensional conducting states, predicted by Schrieffer,[1] was experimentally confirmed by Fowler *et al.*[2] several years ago using surface magnetoresistance measurements on the $n$-type inversion layer of a {100} sili-